ACS Macro Letters

pubs.acs.org/macroletters Letter

Fabrication of Three-Dimensional Polymer-Brush Gradients within Elastomeric Supports by Cu^0-Mediated Surface-Initiated ATRP

Rebecca Faggion Albers, Tommaso Magrini, Matteo Romio, Edson R. Leite, Rafael Libanori, André R. Studart, and Edmondo M. Benetti*

Cite This: *ACS Macro Lett.* 2021, 10, 1099–1106 Read Online

ACCESS | Metrics & More | Article Recommendations | Supporting Information

ABSTRACT: Cu^0-mediated surface-initiated ATRP (Cu^0 SI-ATRP) emerges as a versatile, oxygen-tolerant process to functionalize three-dimensional (3D), microporous supports forming single and multiple polymer-brush gradients with a fully tunable composition. When polymerization mixtures are dispensed on a Cu^0-coated plate, this acts as oxygen scavenger and source of active catalyst. In the presence of an ATRP initiator-bearing microporous elastomer placed in contact with the metallic plate, the reaction solution infiltrates by capillarity through the support, simultaneously triggering the controlled growth of polymer brushes. The polymer grafting process proceeds with kinetics that are determined by the progressive infiltration of the reaction solution within the microporous support and by the continuous diffusion of catalyst regenerated at the Cu^0 surface. The combination of these effects enables the accessible generation of 3D polymer-brush gradients extending across the microporous scaffolds used as supports, finally providing materials with a continuous variation of interfacial composition and properties.

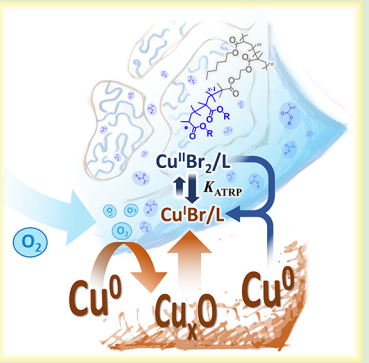

The development of surface-initiated reversible deactivation radical polymerization (SI-RDRP) techniques that are tolerant to oxygen has enabled the translation of the synthesis of polymer brushes into fabrication processes that could potentially lead to industrial applications.[1]

SI-RDRP methods that are compatible with ambient conditions typically encompass the application of oxygen scavengers. These prevent the need for performing long and tedious deoxygenation processes prior to the application of polymerization mixtures on initiator-bearing supports, and thus permit the syntheses of polymer brushes from extremely large substrates.[2−4] Recently applied oxygen scavengers include transition metal complexes coupled to visible/UV light[5] or appropriate reducing agents,[6] enzymes,[7,8] photosensitizers,[9,10] or zerovalent-metal surfaces.[11−14]

The application of zerovalent-metal (Mt^0) plates for surface-initiated atom transfer radical polymerization (Mt^0 SI-ATRP) has been recently demonstrated to enable the rapid fabrication of polymer-brush coatings, on both inorganic and organic surfaces under ambient conditions, and to employ just microliter volumes of reaction mixtures.[15−17]

During Cu^0-mediated SI-ATRP (Cu^0 SI-ATRP), the most widely applied Mt^0 SI-ATRP, a polymerization mixture, including monomer (M), solvent, and transition metal complex-based catalyst in its highest oxidation state (Cu^{II}/L, where L is a generic ligand), is sandwiched between an initiator-bearing substrate and a Cu^0-coated plate. The Cu^0-coated surface consumes oxygen dissolved in the polymerization medium, generating a Cu_xO layer that acts as the source of Cu^{II}/L and Cu^{I}/L species. Simultaneously, Cu^{II}/L species diffusing from the Cu_xO layer and those that were externally added constantly (re)generate Cu^{I}-based activators through comproportionation with Cu^0. When the catalyst diffusing from the metallic plate reaches the ATRP initiator-functionalized substrate, the growth of polymer brushes according to the ATRP equilibrium is eventually triggered.[18]

Following this general mechanism, SI-ATRPs mediated by Cu^0 and, recently, Zn^0 plates were used to fabricate compositionally diverse brushes from model, flat substrates, and different organic supports, including microporous cellulose, elastomers, and hydrogels.[16,17,19] In addition, the growth of polymer brushes under cytocompatible conditions was demonstrated in the case of Fe^0-mediated SI-ATRP.[20]

Through a comprehensive understanding of its mechanism, the groups of Jordan and Benetti demonstrated that Mt^0 SI-ATRP can be additionally applied to fabricate structured coatings across large substrates. For instance, by continuously varying the vertical distance between an ATRP initiator-bearing surface and a Mt^0-coated plate (*i.e.*, by tilting the Mt^0-coated plate), coatings featuring multiple gradients in brush composition and properties could be obtained.[13,14,18] Moreover, micropatterned brush films presenting different polymer

Received: July 6, 2021
Accepted: August 6, 2021
Published: August 11, 2021

https://doi.org/10.1021/acsmacrolett.1c00446
ACS Macro Lett. 2021, 10, 1099–1106

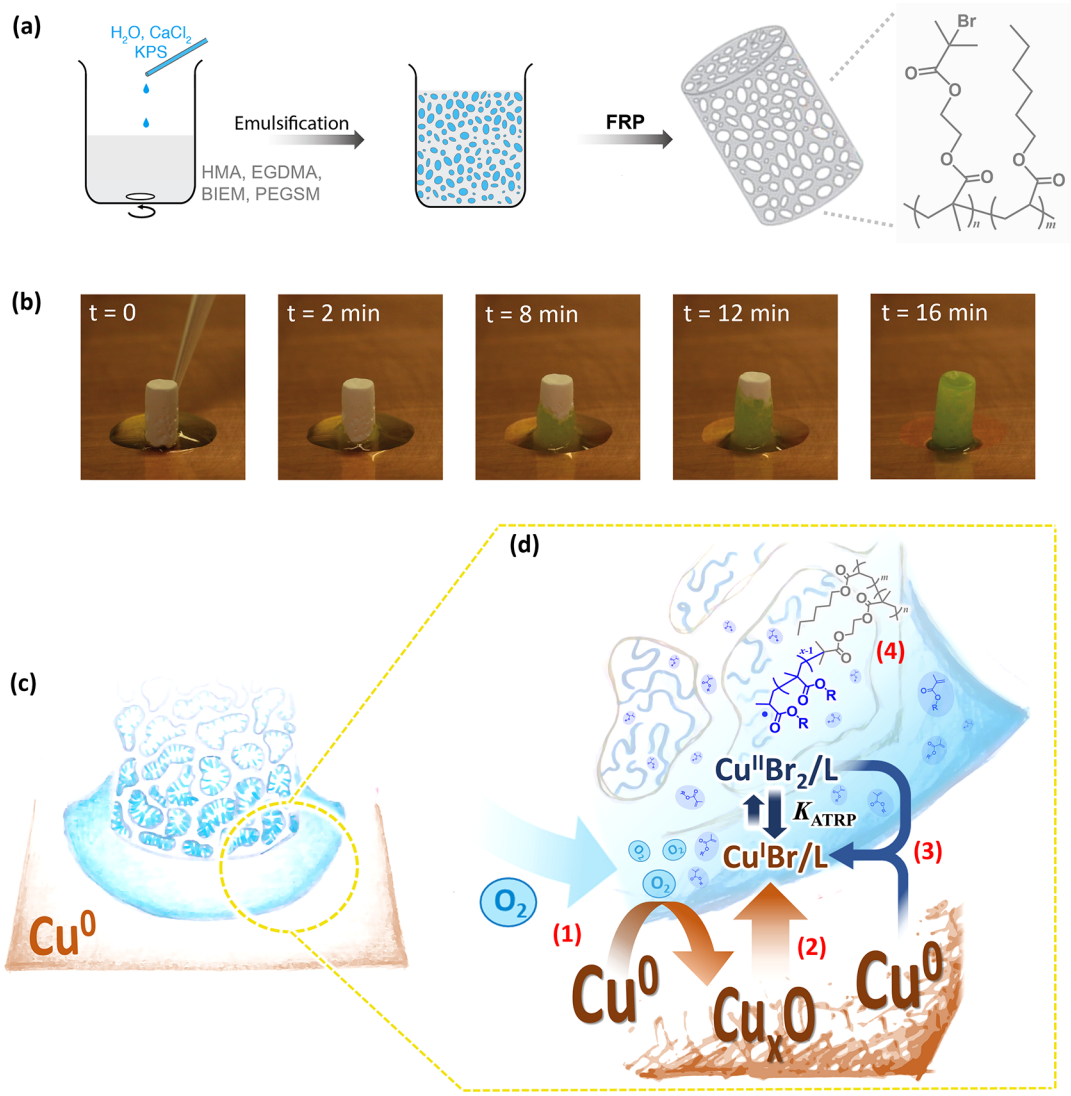

Figure 1. (a) Fabrication of an ATRP initiator-bearing polyHIPE. The HIPE was prepared by mixing an apolar (oil) phase containing HMA (63 mol %), EGDMA (4 mol %), BIEM (17 mol %), and PEGSM (16 mol %), with an aqueous phase including $CaCl_2$ (90 mM) and the free radical initiator KPS (7.4 mM). The ATRP initiator-bearing polyHIPE was obtained through FRP and cross-linking of the HIPE, followed by Soxhlet extraction with acetone, solvent exchange to water, and freeze-drying. (b) A polymerization mixture containing monomer (M), solvent, ligand (L), and $Cu^{II}Br_2$ was dispensed on an activated Cu^0-coated surface, and the polyHIPE was placed in contact with it. Complete infiltration of the polymerization mixture through the polyHIPE required ~16 min. (c, d) Mechanism of Cu^0 SI-ATRP from ATRP initiator-bearing polyHIPEs. (1) Oxygen is consumed by the Cu^0 surface through the formation of a Cu_xO layer, which acts (2) as the source of catalyst; (3) Cu^I/L activators are continuously (re)generated by comproportionation between Cu^0 and Cu^{II}/L species; the growth of polymer grafts (4) within the pores proceeds according to the ATRP equilibrium.

compositions could be synthesized with the aid of microfluidics.[21]

Motivated by the versatility and the widespread applicability of Mt^0 SI-ATRP for the chemical and morphological structuring of polymer brush coatings on two-dimensional (2D) substrates, in this work, we concentrated on applying this technique for functionalizing three-dimensional (3D) supports in a spatially controlled fashion.

The 3D supports used as starting platforms for the growth of chemically different brushes are microporous elastomers obtained by cross-linking poly(high internal phase emulsion)s (polyHIPEs).[22] These were obtained by vigorously mixing an apolar phase, which contained the ATRP inimer 2-(2-bromoisobutyryloxy)ethyl methacrylate (BIEM; 17 mol %),[23] hexyl methacrylate (HMA, 63 mol %), ethylene glycol dimethacrylate (EGDMA, 4 mol %), and poly(ethylene glycol) sorbitan monooleate (PEGSM, 16 mol %), with an aqueous phase containing $CaCl_2$ (90 mM) and the free radical initiator potassium persulfate (KPS, 7.4 mM; Figure 1a).

Free radical polymerization (FRP) and cross-linking of the generated emulsion were induced by heating at 80 °C overnight to yield a highly porous, elastomeric 3D structure (Figure 1a), which included ATRP initiator functions (Figure S2).

The obtained polyHIPEs were subsequently used as supports for Cu^0 SI-ATRP. Following a typical polymer grafting process, which is depicted in Figure 1b,c, 125 μL of a polymerization mixture containing ligand, $Cu^{II}Br_2$, monomer, and solvent was dispensed on a Cu^0 plate, which was previously "activated" by chemically removing the oxide layer that spontaneously formed on it (Supporting Information). A cylindrical polyHIPE with a height of 8 mm and a base of 13

https://doi.org/10.1021/acsmacrolett.1c00446
ACS Macro Lett. 2021, 10, 1099−1106

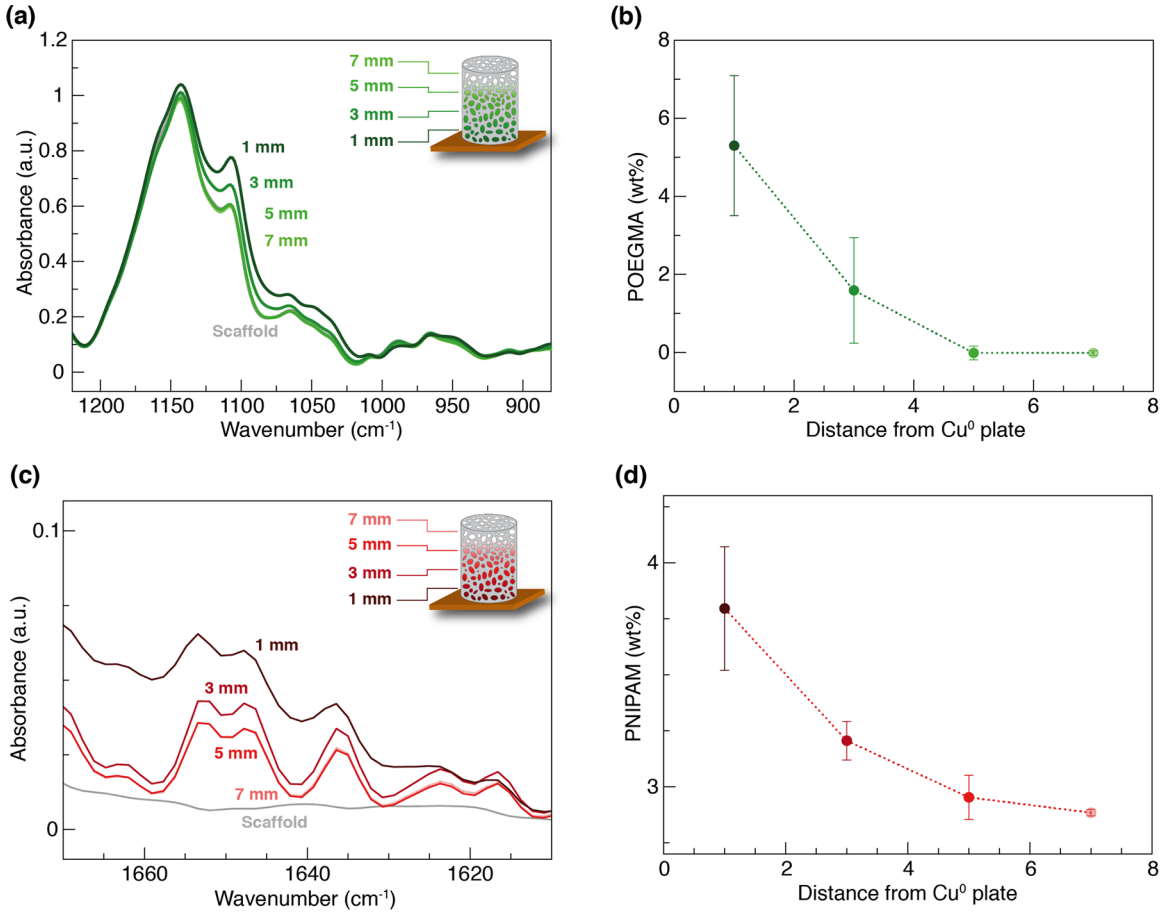

Figure 2. (a) ATR-IR spectra of polyHIPE recorded at positions that were kept at different distances (1, 3, 5, and 7 mm) from the Cu^0 plate during Cu^0 SI-ATRP of OEGMA. (b) Relative content (wt %) of POEGMA brushes recorded at different positions across the polyHIPE following Cu^0 SI-ATRP. (c) ATR-IR spectra recorded at different positions across a polyHIPE (1, 3, 5, and 7 mm) from the Cu^0 surface during Cu^0 SI-ATRP of NIPAM. (d) Relative content (wt %) of PNIPAM brushes across a brush-functionalized polyHIPE.

mm^2 was subsequently placed in contact with the polymerization solution, and the whole Cu^0 SI-ATRP setup was immediately positioned within a closed desiccator connected to a balloon full of Ar, in this way, generating an environment presenting a limited amount of oxygen.

The polymerization mixture rapidly infiltrated into the microporous structure of the polyHIPE due to capillary forces.[24] Simultaneously, direct contact between the reaction mixture and the Cu^0 plate led to the consumption of O_2 and the concomitant formation of a Cu_xO layer on the metallic surface.

Within this setup (Figure 1c,d), Cu^I/L-based activators are generated both by diffusion of Cu^I species from the newly formed oxide layer in the presence of complexing L[15,18] and due to comproportionation between Cu^{II}/L species and Cu^0.[25−28] Cu^I/L species are transported with the polymerization solution through the microporous scaffold and trigger the growth of polymer brushes from initiator sites that are exposed on the surface of pores, which proceeds according to the ATRP equilibrium (Figure 1d).

Generally, two main parameters are expected to regulate the formation of a brush gradient within the 3D supports via Cu^0 SI-ATRP. On the one hand, the progressive and relatively quick infiltration of the reaction mixture determines different polymerization times within a polyHIPE. On the other hand, the presence of a Cu^0 plate that is left in contact with one side of the microporous support triggers the formation of Cu^I/L activators and their slow diffusion, as it was described in detail previously.[18]

The vertical distance between a specific pore and the Cu^0 plate (where the reaction mixture is initially dispensed) determines the contact time between the mixture and the reactive sites. Hence, ATRP initiators that are closer to the plate are in contact for longer times with the polymerization solution and, thus, can generate brushes with relatively higher molar masses compared to those grown from sites further away from the bottom of the microporous scaffold.

Simultaneously, the concentration of Cu^I/L activators progressively decreases with the distance from the metallic plate, where these are constantly (re)generated through comproportionation. This phenomenon induces a local increase of $[Cu^I/L]/[Cu^{II}/L]$ close to the metallic surface and, thus, an increment in the polymerization rate,[29] which is expected to follow a progressive decay across the polyHIPE when this is fully infiltrated by the mixture.

The combined effects of progressive variations in polymerization time and rate resulted in the formation of a polymer-brush gradient across the polyHIPE. However, it is important to emphasize that the infiltration of polyHIPEs by the reaction mixtures and the diffusion of Cu^I/L species continuously (re)generated at the Cu^0 plate are phenomena taking place at different time scales. In the first case, complete infiltration

https://doi.org/10.1021/acsmacrolett.1c00446
ACS Macro Lett. 2021, 10, 1099−1106

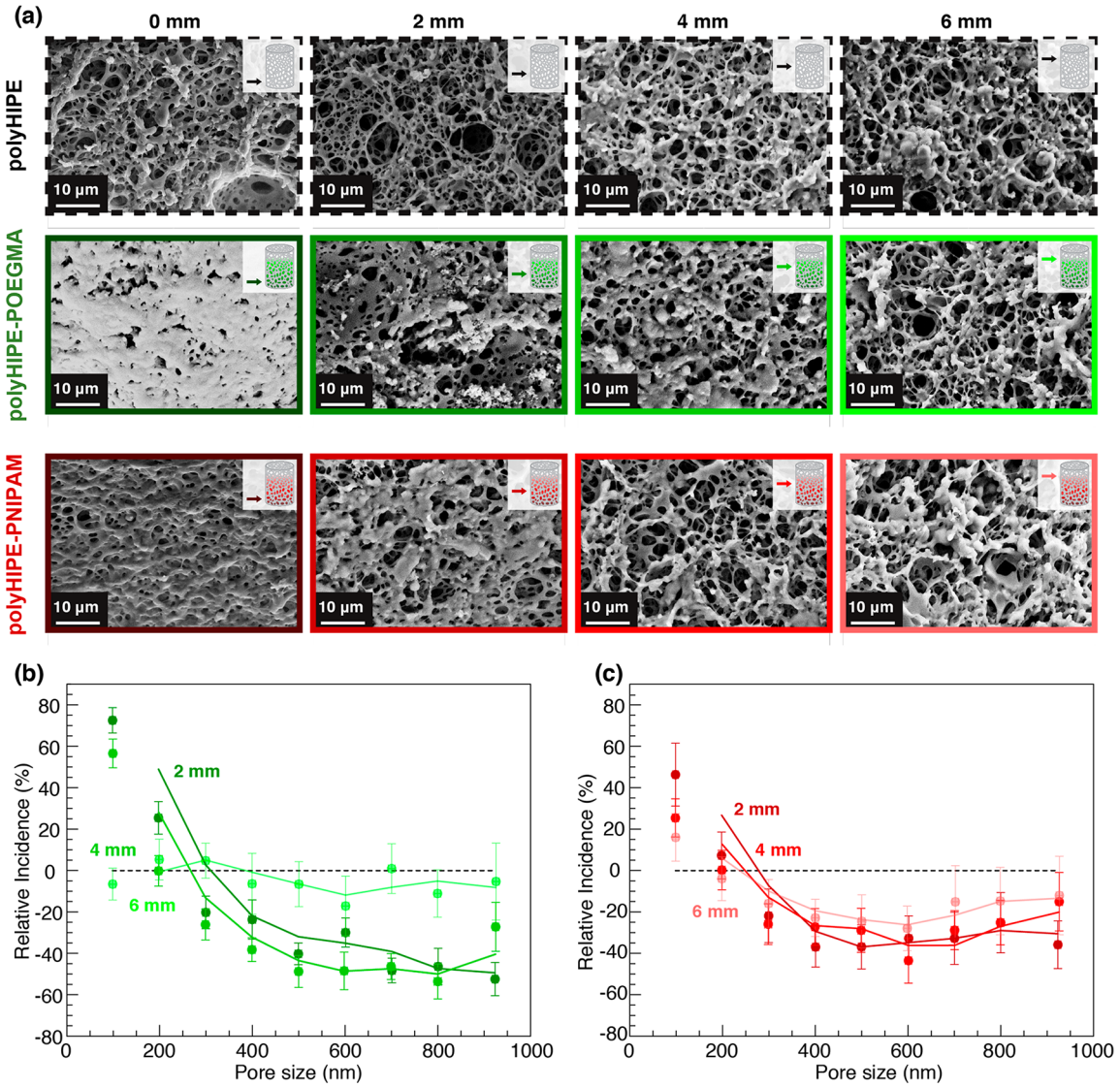

Figure 3. (a) SEM micrographs of the polyHIPE before (dashed black frame) and after functionalization with POEGMA (green frame) and PNIPAM (red frame) brushes. The micrographs were recorded at different positions across the main axis of the supports, namely, at 0, 2, 4, and 6 mm of the distance from the Cu^0 plate. Pore size distributions within polyHIPEs following the growth of (b) POEGMA and (c) PNIPAM brushes.

requires just minutes. In the second case, diffusion of the catalyst within the already infiltrated polyHIPEs is much slower, typically occurring at rates <1 mm h^{-1}.[18]

Hence, considering that at the typical polymerization rates attained by Cu^0 SI-ATRP in organic solvents, brush growth proceeds at 10−20 nm h^{-1}, the relatively fast infiltration process is expected to play a non-negligible, but minor role in determining the formation of brush gradients. In contrast, diffusion of activators, which occurs at time scales similar to those relevant for brush growth, is expected to be the major determinant for the formation of graded brushes across the supports.

The formation of a single 3D gradient of poly-[(oligoethylene glycol) methacrylate] (POEGMA) brushes within an ATRP initiator-bearing polyHIPE is exemplarily described.

A polymerization mixture (125 μL) containing OEGMA (25% v/v) in dimethylformamide (DMF), 10 mM tris(2-pyridylmethyl)amine (TPMA), and 10 mM $Cu^{II}Br_2$ was poured on a freshly activated Cu^0 plate. A polyHIPE presenting a cylindrical shape was immediately placed on the drop of this reaction mixture, and the entire setup was closed inside a desiccator connected with a balloon filled with Ar. The progressive infiltration of the polymerization mixture, which presented a pale green color, within the colorless, microporous structure could be clearly visualized, and it was typically quick, with the entire support getting filled up within just ∼16 min (Figure 1b). To generate a POEGMA brush gradient, the polyHIPE was incubated on the Cu^0 plate for an overall time of 5 h, after which the support was extensively rinsed by Soxhlet extraction in acetone, later swollen in ultra-pure water, and finally freeze-dried.

The formation of a 3D POEGMA-brush gradient was verified by attenuated total reflection infrared (ATR-IR) spectroscopy, which was used to record the composition of the microporous elastomer at different positions along its main axis, namely, 1, 3, 5, and 7 mm away from the contact area with the Cu^0 plate (Figure 2a).

All ATR-IR spectra were normalized with respect to the band at 1728 cm^{-1} correlated to the stretching of C═O

https://doi.org/10.1021/acsmacrolett.1c00446
ACS Macro Lett. 2021, 10, 1099−1106

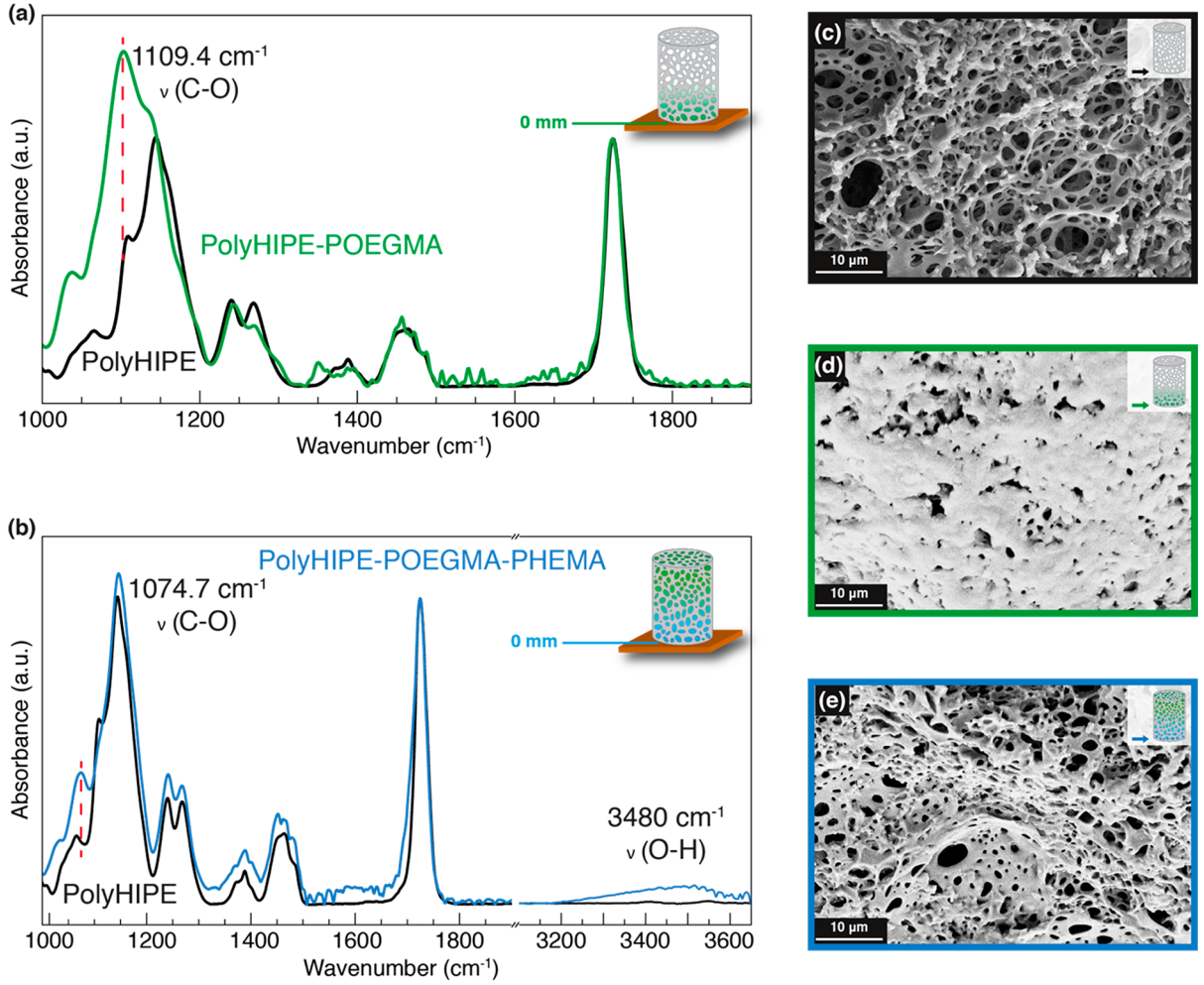

Figure 4. (a) ATR-IR spectra of polyHIPE before (black trace) and after (green trace) the growth of POEGMA brushes (yielding polyHIPE-POEGMA). The spectrum of polyHIPE-POEGMA was recorded on the side of the elastomer that was in contact with the Cu^0 plate during Cu^0 SI ATRP. (b) ATR-IR spectra of polyHIPE-POEGMA before (black trace) and after (blue trace) Cu^0 SI-ATRP of HEMA (which yielded polyHIPE-POEGMA-PHEMA). (c) SEM micrograph of unfunctionalized polyHIPE. (d) SEM micrograph of polyHIPE-POEGMA, recorded on the side of the elastomer that was in contact with the Cu^0 plate during Cu^0 SI ATRP of OEGMA. (e) SEM micrograph of polyHIPE-POEGMA-PHEMA, recorded on the portion of the elastomer that was in contact with the Cu^0 plate during Cu^0 SI ATRP of HEMA.

groups, which are included both in the repeating units of the polymer forming the support and in POEGMA brushes.

Following Cu^0 SI-ATRP, the appearance of the band at 1109.4 cm^{-1}, corresponding to the C—O stretching of the ether moieties along the OEGMA side chains, confirmed the successful growth of POEGMA brushes. The relative intensity of this specific signal gradually decreased with increasing the distance from the Cu^0 plate, indicating that the pores closer to the metallic plate were functionalized with higher-molar-mass brushes compared to those further away from it (Figure 2a) and, thus, confirming the formation of a brush gradient across the elastomer. Calibration of the ATR-IR data (Figure S3) enabled to quantitatively estimate the relative amount of POEGMA brushes across the polyHIPE, which varied between 0 and 7 wt % across 7 mm of distance from the Cu^0 plate (Figure 2b).

Chemically different 3D brush gradients could be easily fabricated by varying the composition of the polymerization mixture. Following a similar procedure as the one reported above, poly(*N*-isopropylacrylamide) (PNIPAM) brush gradients were obtained by placing an ATRP initiator-bearing polyHIPE on a Cu^0 plate previously wetted with 125 μL of a mixture comprising 3 M NIPAM in DMF, 10 mM TPMA, and 10 mM $Cu^{II}Br_2$.

After 4 h, during which the infiltrated support was left in contact with the Cu^0 plate, the functionalized elastomer was thoroughly rinsed by Soxhlet extraction in acetone, swollen in ultra-pure water, and freeze-dried. ATR-IR revealed the presence of PNIPAM grafts, through the appearance of a clear band at 1646 cm^{-1}, which originated from the C═O stretching of the amide groups of the polymer. Opportune calibration (Figure S4) enabled the quantification of the relative content of PNIPAM brushes, which varied between 2 and 4 wt % across the functionalized support. The amount of PNIPAM brushes progressively decreased between the portion of the elastomer that had been in contact with the metallic plate and the volumes that had been at ∼7 mm of vertical distance from it during Cu^0 SI-ATRP.

The generation of POEGMA and PNIPAM brush gradients within polyHIPEs was further confirmed by analyzing scanning electron microscopy (SEM) images recorded across functionalized supports at positions that were kept at different distances from the metallic surface during Cu^0 SI-ATRP. Because Cu^0 SI-ATRP induced the growth of brushes within the pores, the

https://doi.org/10.1021/acsmacrolett.1c00446
ACS Macro Lett. 2021, 10, 1099−1106

formation of brush gradients could be monitored through a simultaneous, gradual variation in the pore-size distributions across the supports.

As reported in Figure 3a, both POEGMA and PNIPAM brushes almost completely filled the pores of the elastomeric structures where these were in direct contact with the Cu^0 plates (positions 0 mm, as indicated in Figure 3a).

Assuming that any change in porosity after Cu^0 SI-ATRP was exclusively due to the growth of polymer grafts, the presence of brushes at a given vertical distance from the Cu^0 plate >0 mm could be recorded as a change in pore size with respect to the pristine, unfunctionalized support.

As reported in Figure 3, following Cu^0 SI-ATRP, pore-size distributions progressively shifted toward a greater relative incidence of small pores due to the growth of POEGMA (Figure 3b) and PNIPAM (Figure 3c) brushes. The presence of smaller pores is especially highlighted in positions that were close to the metallic plate during Cu^0 SI-ATRP (2 and 4 mm of vertical distances), while the porosity of functionalized polyHIPEs gradually approximated that recorded on pristine supports at a distance of 6 mm.

In the case of POEGMA, the brush gradient extended within the scaffold across ∼4 mm from the contact with the Cu^0 plate. In contrast, the PNIPAM brush gradient seemed to develop through the whole volume of the polyHIPE, with pores relatively far away from the Cu^0 surface still being functionalized with PNIPAM grafts.

Hence, the combination of ATR-IR and SEM analyses demonstrated the formation of POEGMA- and PNIPAM-brush gradients within microporous polyHIPEs. In the former case, brush gradients presented a "steeper" morphology, with a more marked variation in brush-molar mass across relatively small distances. In the latter case, PNIPAM brush gradients showed a less pronounced variation in brush properties, and extended across the entire support. This phenomenon was presumably due to the faster kinetics of Cu^0 SI-ATRP of NIPAM, which determined the formation of high-molar-mass grafts already after relatively short incubation times in the reaction mixture.[15]

The application of Cu^0 SI-ATRP on initiator-bearing polyHIPEs additionally enabled the fabrication of multiple brush gradients within the same support. This is especially relevant, as 3D polymeric matrices including brushes featuring graded variations in functionalities and properties could be employed as suitable supports for a variety of applications, including cell-culture platforms, tissue engineering supports, and fully synthetic prostheses.[30]

Multiple brush gradients could be easily generated if the general functionalization procedure described for a single brush gradient was repeated, for example, by turning upside down a brush-functionalized polyHIPE after a first Cu^0 SI-ATRP step and subjecting it to the diffusion of a reaction mixture containing a different monomer.

For instance, a polyHIPE featuring a POEGMA brush 3D gradient (polyHIPE-POGEMA) was subjected to an additional Cu^0 SI-ATRP step to generate a second brush gradient of poly(2-hydroxylethyl methacrylate) (PHEMA) in the opposite direction along the main axis of the elastomeric support (yielding polyHIPE-POEGMA-PHEMA; Figure 4).

Following a similar protocol as that reported above, 125 μL of polymerization mixture containing 25% v/v HEMA in DMF, 10 mM TPMA, and 10 mM $Cu^{II}Br_2$ was dispensed on an activated Cu^0 surface. A previously prepared polyHIPE-POEGMA was turned upside down and placed on the dropped solution, with the side that was left unfunctionalized during the first Cu^0 SI-ATRP step now facing the metallic plate. The new reaction mixture was left diffusing inside the polyHIPE-POEGMA for 2 h, after which the support was rinsed by Soxhlet extraction in acetone, swollen in ultrapure water, and again freeze-dried.

ATR-IR and SEM confirmed the formation of a double brush gradient. As reported in Figure 4a, following Cu^0 SI-ATRP of OEGMA, the appearance of a strong band at 1109.4 cm^{-1}, corresponding to C—O stretching, confirmed the presence of high-molar-mass POEGMA grafts at one side of the polyHIPE. This was confirmed by SEM (Figure 4d), which highlighted how POEGMA brushes nearly completely filled the pores of the polyHIPE where this was contacting the Cu^0 plate. After Cu^0 SI-ATRP of HEMA, the ATR-IR spectrum recorded on the opposite side of the polyHIPE showed the appearance of the bands at 1074.7 cm^{-1} from C—O stretching and 3480 cm^{-1} from O—H stretching, confirming the successful growth of PHEMA brushes (Figure 4b). This result was corroborated by the SEM micrographs recorded on the same areas of the polyHIPE, which suggested the presence of brushes covering the pores of the support (Figure 4e).

These results demonstrated that Cu^0 SI-ATRP represents an efficient process not only to generate structured polymer brushes from 2D substrates[31] but also to functionalize 3D supports in a controlled fashion, forming single and multiple brush gradients with a fully tunable composition. It is important to emphasize that even when applied on 3D supports, Cu^0 SI-ATRP could be performed without the need for deoxygenation of the polymerization mixtures and enabled the controlled growth of brushes also in the presence of a limited content of oxygen. These attractive features further confirmed the versatility of this polymerization process for the synthesis of polymer brush coatings from multidimensional materials and the possibility to translate it into upscalable functionalization techniques.

■ ASSOCIATED CONTENT

Supporting Information

The Supporting Information is available free of charge at https://pubs.acs.org/doi/10.1021/acsmacrolett.1c00446.

Materials, experimental procedures, and NMR and ATR-IR characterizations (PDF)

■ AUTHOR INFORMATION

Corresponding Author

Edmondo M. Benetti − *Laboratory for Surface Science and Technology, Department of Materials, ETH Zürich, CH-8093 Zurich, Switzerland; Swiss Federal Laboratories for Materials Science and Technology (Empa), St. Gallen, Switzerland; Department of Chemical Sciences, University of Padova, 35131 Padova, Italy;* orcid.org/0000-0002-5657-5714; Email: edmondo.benetti@unipd.it

Authors

Rebecca Faggion Albers − *Complex Materials, Department of Materials, ETH Zürich, CH-8093 Zurich, Switzerland; Laboratory for Surface Science and Technology, Department of Materials, ETH Zürich, CH-8093 Zurich, Switzerland; Swiss Federal Laboratories for Materials Science and Technology (Empa), St. Gallen, Switzerland; Department of*

https://doi.org/10.1021/acsmacrolett.1c00446
ACS Macro Lett. 2021, 10, 1099−1106

Chemistry, Federal University of São Carlos, 13565-905 São Carlos, SP, Brazil; Brazilian Nanotechnology National Laboratory (LNNano), Brazilian Center for Research in Energy and Materials (CNPEM), 13083-970 Campinas, Brazil; orcid.org/0000-0001-5263-2980

Tommaso Magrini − *Complex Materials, Department of Materials, ETH Zürich, CH-8093 Zurich, Switzerland*

Matteo Romio − *Laboratory for Surface Science and Technology, Department of Materials, ETH Zürich, CH-8093 Zurich, Switzerland; Swiss Federal Laboratories for Materials Science and Technology (Empa), St. Gallen, Switzerland*

Edson R. Leite − *Department of Chemistry, Federal University of São Carlos, 13565-905 São Carlos, SP, Brazil; Brazilian Nanotechnology National Laboratory (LNNano), Brazilian Center for Research in Energy and Materials (CNPEM), 13083-970 Campinas, Brazil*

Rafael Libanori − *Complex Materials, Department of Materials, ETH Zürich, CH-8093 Zurich, Switzerland;* orcid.org/0000-0003-3965-6974

André R. Studart − *Complex Materials, Department of Materials, ETH Zürich, CH-8093 Zurich, Switzerland;* orcid.org/0000-0003-4205-8545

Complete contact information is available at: https://pubs.acs.org/10.1021/acsmacrolett.1c00446

Notes

The authors declare no competing financial interest.

■ ACKNOWLEDGMENTS

We thank Prof. Katharina Maniura (EMPA) for the fruitful scientific discussions. We acknowledge Empa and the Brazilian agency Fundação de Amparo à Pesquisa do Estado de São Paulo-FAPESP (2016/14493-7 and 2017/22304-2) for the financial support.

■ REFERENCES

(1) Yeow, J.; Chapman, R.; Gormley, A. J.; Boyer, C. Up in the Air: Oxygen Tolerance in Controlled/Living Radical Polymerisation. *Chem. Soc. Rev.* **2018**, *47*, 4357−4387.

(2) Dunderdale, G. J.; Urata, C.; Miranda, D. F.; Hozumi, A. Large-Scale and Environmentally Friendly Synthesis of PH-Responsive Oil-Repellent Polymer Brush Surfaces under Ambient Conditions. *ACS Appl. Mater. Interfaces* **2014**, *6*, 11864−11868.

(3) Dunderdale, G. J.; England, M. W.; Urata, C.; Hozumi, A. Polymer Brush Surfaces Showing Superhydrophobicity and Air-Bubble Repellency in a Variety of Organic Liquids. *ACS Appl. Mater. Interfaces* **2015**, *7*, 12220−12229.

(4) Sato, T.; Dunderdale, G. J.; Urata, C.; Hozumi, A. Sol-Gel Preparation of Initiator Layers for Surface-Initiated ATRP: Large-Scale Formation of Polymer Brushes Is Not a Dream. *Macromolecules* **2018**, *51*, 10065−10073.

(5) Yan, W.; Dadashi-Silab, S.; Matyjaszewski, K.; Spencer, N. D.; Benetti, E. M. Surface-Initiated Photoinduced ATRP: Mechanism, Oxygen Tolerance, and Temporal Control during the Synthesis of Polymer Brushes. *Macromolecules* **2020**, *53*, 2801.

(6) Matyjaszewski, K.; Dong, H.; Jakubowski, W.; Pietrasik, J.; Kusumo, A. Grafting from Surfaces for "Everyone": ARGET ATRP in the Presence of Air. *Langmuir* **2007**, *23*, 4528−4531.

(7) Navarro, L. A.; Enciso, A. E.; Matyjaszewski, K.; Zauscher, S. Enzymatically Degassed Surface-Initiated Atom Transfer Radical Polymerization with Real-Time Monitoring. *J. Am. Chem. Soc.* **2019**, *141*, 3100−3109.

(8) Divandari, M.; Pollard, J.; Dehghani, E.; Bruns, N.; Benetti, E. M. Controlling Enzymatic Polymerization from Surfaces with Switchable Bioaffinity. *Biomacromolecules* **2017**, *18*, 4261−4270.

(9) Narupai, B.; Page, Z. A.; Treat, N. J.; McGrath, A. J.; Pester, C. W.; Discekici, E. H.; Dolinski, N. D.; Meyers, G. F.; Read de Alaniz, J.; Hawker, C. J. Simultaneous Preparation of Multiple Polymer Brushes under Ambient Conditions Using Microliter Volumes. *Angew. Chem., Int. Ed.* **2018**, *57*, 13433−13438.

(10) Li, M.; Fromel, M.; Ranaweera, D.; Rocha, S.; Boyer, C.; Pester, C. W. SI-PET-RAFT Surface-Initiated Photoinduced Electron Transfer-Reversible Addition-Fragmentation Chain Transfer Polymerization. *ACS Macro Lett.* **2019**, *8*, 374−380.

(11) Mohamadnia, Z.; Ahmadi, E.; Ghasemnejad, M.; Hashemikia, S.; Doustgani, A. Surface Modification of Mesoporous Nanosilica with [3-(2-Aminoethylamino) Propyl] Trimethoxysilane and Its Application in Drug Delivery. *Mater. Sci. Eng., C* **2015**, *11*, 167−177.

(12) Zhang, T.; Du, Y.; Kalbacova, J.; Schubel, R.; Rodriguez, R. D.; Chen, T.; Zahn, D. R. T.; Jordan, R. Wafer-Scale Synthesis of Defined Polymer Brushes under Ambient Conditions. *Polym. Chem.* **2015**, *6*, 8176−8183.

(13) Dehghani, E. S.; Du, Y.; Zhang, T.; Ramakrishna, S. N.; Spencer, N. D.; Jordan, R.; Benetti, E. M. Fabrication and Interfacial Properties of Polymer Brush Gradients by Surface-Initiated Cu(0)-Mediated Controlled Radical Polymerization. *Macromolecules* **2017**, *50*, 2436−2446.

(14) Zhang, T.; Du, Y.; Müller, F.; Amin, I.; Jordan, R. Surface-Initiated Cu(0) Mediated Controlled Radical Polymerization (SI-CuCRP) Using a Copper Plate. *Polym. Chem.* **2015**, *6* (14), 2726−2733.

(15) Yan, W.; Fantin, M.; Spencer, N. D.; Matyjaszewski, K.; Benetti, E. M. Translating Surface-Initiated Atom Transfer Radical Polymerization into Technology: The Mechanism of Cu^0-Mediated SI-ATRP under Environmental Conditions. *ACS Macro Lett.* **2019**, *8*, 865−870.

(16) Yan, W.; Fantin, M.; Ramakrishna, S.; Spencer, N. D.; Matyjaszewski, K.; Benetti, E. M. Growing Polymer Brushes from a Variety of Substrates under Ambient Conditions by Cu^0-Mediated Surface-Initiated ATRP. *ACS Appl. Mater. Interfaces* **2019**, *11*, 27470−27477.

(17) Zhang, K.; Yan, W.; Simic, R.; Benetti, E. M.; Spencer, N. D. Versatile Surface Modification of Hydrogels by Surface-Initiated, Cu^0-Mediated Controlled Radical Polymerization. *ACS Appl. Mater. Interfaces* **2020**, *12*, 6761−6767.

(18) Fantin, M.; Ramakrishna, S. N.; Yan, J.; Yan, W.; Divandari, M.; Spencer, N. D.; Matyjaszewski, K.; Benetti, E. M. The Role of Cu^0 in Surface-Initiated Atom Transfer Radical Polymerization: Tuning Catalyst Dissolution for Tailoring Polymer Interfaces. *Macromolecules* **2018**, *51*, 6825−6835.

(19) Faggion Albers, R.; Yan, W.; Romio, M.; Leite, E. R.; Spencer, N. D.; Matyjaszewski, K.; Benetti, E. M. Mechanism and Application of Surface-Initiated ATRP in the Presence of a Zn^0 plate. *Polym. Chem.* **2020**, *11*, 7009−7014.

(20) Layadi, A.; Kessel, B.; Yan, W.; Romio, M.; Spencer, N. D.; Zenobi-Wong, M.; Matyjaszewski, K.; Benetti, E. M. Oxygen Tolerant and Cytocompatible Iron(0)-Mediated ATRP Enables the Controlled Growth of Polymer Brushes from Mammalian Cell Cultures. *J. Am. Chem. Soc.* **2020**, *142*, 3158−3164.

(21) Li, W.; Sheng, W.; Wegener, E.; Du, Y.; Li, B.; Zhang, T.; Jordan, R. Capillary Micro Fluidic-Assisted Surface Structuring. *ACS Macro Lett.* **2020**, *9*, 328−333.

(22) Kimmins, S. D.; Cameron, N. R. Functional Porous Polymers by Emulsion Templating: Recent Advances. *Adv. Funct. Mater.* **2011**, *21*, 211−225.

(23) Matyjaszewski, K.; Pyun, J.; Gaynor, S. G. Preparation of Hyperbranched Polyacrylates by Atom Transfer Radical Polymerization, 4: The Use of Zero-Valent Copper. *Macromol. Rapid Commun.* **1998**, *19*, 665−670.

(24) Gunnewiek, M. K.; Di Luca, A.; Bollemaat, H. Z.; van Blitterswijk, C. A.; Vancso, G. J.; Moroni, L.; Benetti, E. M. Creeping Proteins in Microporous Structures: Polymer Brush-Assisted Fab-

rication of 3D Gradients for Tissue Engineering. *Adv. Healthcare Mater.* **2015**, *4* (8), 1169−1174.
(25) Konkolewicz, D.; Wang, Y.; Zhong, M.; Krys, P.; Isse, A. A.; Gennaro, A.; Matyjaszewski, K. Reversible-Deactivation Radical Polymerization in the Presence of Metallic Copper. A Critical Assessment of the SARA ATRP and SET-LRP Mechanisms. *Macromolecules* **2013**, *46*, 8749−8772.
(26) Augustine, K. F.; Ribelli, T. G.; Fantin, M.; Krys, P.; Cong, Y.; Matyjaszewski, K. Activation of Alkyl Halides at the Cu^0 Surface in SARA ATRP: An Assessment of Reaction Order and Surface Mechanisms. *J. Polym. Sci., Part A: Polym. Chem.* **2017**, *55*, 3048−3057.
(27) Konkolewicz, D.; Wang, Y.; Krys, P.; Zhong, M.; Isse, A. A.; Gennaro, A.; Matyjaszewski, K. SARA ATRP or SET-LRP. End of Controversy? *Polym. Chem.* **2014**, *5*, 4409−4417.
(28) Konkolewicz, D.; Krys, P.; Góis, J. R.; Mendonça, P. V.; Zhong, M.; Wang, Y.; Gennaro, A.; Isse, A. A.; Fantin, M.; Matyjaszewski, K. Aqueous RDRP in the Presence of Cu^0: The Exceptional Activity of CuI Confirms the SARA ATRP Mechanism. *Macromolecules* **2014**, *47*, 560−570.
(29) Jeyaprakash, J. D.; Samuel, S.; Dhamodharan, R.; Rühe, J. Polymer Brushes via ATRP: Role of Activator and Deactivator in the Surface-Initiated ATRP of Styrene on Planar Substrates. *Macromol. Rapid Commun.* **2002**, *23*, 277−281.
(30) Benetti, E. M.; Gunnewiek, M. K.; Van Blitterswijk, C. A.; Julius Vancso, G.; Moroni, L. Mimicking Natural Cell Environments: Design, Fabrication and Application of Bio-Chemical Gradients on Polymeric Biomaterial Substrates. *J. Mater. Chem. B* **2016**, *4*, 4244−4257.
(31) Zhang, T.; Benetti, E. M.; Jordan, R. Surface-Initiated Cu(0)-Mediated CRP for the Rapid and Controlled Synthesis of Quasi-3D Structured Polymer Brushes. *ACS Macro Lett.* **2019**, *8*, 145−153.

https://doi.org/10.1021/acsmacrolett.1c00446
ACS Macro Lett. 2021, 10, 1099−1106